

# Hierarchical copper/nickel-based manganese dioxide core-shell nanostructure for supercapacitor electrodes



Hao Chen<sup>a</sup>, Xue Qiang Qi<sup>b,\*\*</sup>, Min Kuang<sup>a</sup>, Fan Dong<sup>c</sup>, Yu Xin Zhang<sup>a,d,\*</sup>

<sup>a</sup> College of Material Science and Engineering, Chongqing University, Chongqing 400044, PR China

<sup>b</sup> College of Chemistry and Chemical Engineering, Chongqing University, Chongqing 400044, PR China

<sup>c</sup> Chongqing Key Laboratory of Catalysis and Functional Organic Molecules, College of Environmental and Biological Engineering, Chongqing Technology and Business University, Chongqing 400067, PR China

<sup>d</sup> National Key Laboratory of Fundamental Science of Micro/Nano-Devices and System Technology, Chongqing University, Chongqing 400044, PR China

## ARTICLE INFO

### Article history:

Received 8 December 2015

Received in revised form 25 June 2016

Accepted 5 July 2016

Available online 6 July 2016

### Keywords:

Manganese dioxides

Nanocomposites

Core-shell nanostructure

Supercapacitor

## ABSTRACT

A novel copper/nickel-based manganese dioxide core-shell nanostructure can be prepared for supercapacitor electrodes using facile hydrothermal methods. Attributed to Kirkendall-type diffusion process, the “core” can transfer to hollow structure during the reaction interestingly. The faradic reaction occurs effectively in the electrode and electrolyte due to the high conductivity of Cu/Ni and large hollow channel structure. As a result, the electrode displays a high specific capacitance ( $374 \text{ F g}^{-1}$  at current density of  $0.25 \text{ A g}^{-1}$ ), fine cycling stability (86.9% retention after 3000 cycles) and outstanding rate capability. These interesting findings suggest that the hybrid material can be a promising candidate for supercapacitor electrodes.

© 2016 Elsevier Ltd. All rights reserved.

## 1. Introduction

With the ever-increasing fossil fuels consumption, energy crisis has become more and more severe in the planet. Large amounts of energy storage technologies are emerging to solve this trouble [1–5]. Supercapacitors, with the features of high power density, fast charge-discharge characteristic and long cycling lifespan, play a potential role in energy storage devices [6–8]. These stunning properties are directly affected by the electrode materials. Based on the previous studies, electrode materials can be divided into three major types: (i) carbon materials, (ii) transition metal oxides, and (iii) conducting polymers [9–13]. Among these electrode materials, transition metal oxides ( $\text{MnO}_2$ ,  $\text{Co}_3\text{O}_4$ ,  $\text{NiO}$  etc.) have drawn extensive research interests due to their advantages of low cost, simple operation, abundance and efficient Faradaic reaction [14–16].

$\text{MnO}_2$  with different morphologies and structures has been investigated widely on account of many excellent characteristics, but most  $\text{MnO}_2$  materials constantly suffers from poor electrical

conductivity ( $10^{-5}$ – $10^{-6} \text{ S cm}^{-1}$ ) and agglomeration [17]. Because of these deficiencies,  $\text{MnO}_2$  is arduous to be effectively utilized during Faradaic reactions. In other words, single-component nanomaterials can hardly satisfy the demand of pleasurable electrochemical performances for supercapacitors. To improve these issues,  $\text{MnO}_2$  is used to combine with other materials to increase electrical conductivity or design rational structures for favorable electrochemical properties. Based on these facts, numerous  $\text{MnO}_2$ -based materials with different structures have been fabricated for supercapacitor electrodes, such as graphene@ $\text{MnO}_2$  [18], carbon nanotubes@ $\text{MnO}_2$  [19,20],  $\text{CuO@MnO}_2$  [21],  $\text{Co}_3\text{O}_4@\text{MnO}_2$  [22,23] nanocomposites. The electrochemical performances of these nanocomposites are effectively enhanced by the synergistic effect. Despite these improvements, it still remains a challenge to develop smart recombination and rational design for electrode materials with specific structure.

Herein, we report a novel copper/nickel-based manganese dioxide core-shell nanostructure for supercapacitor electrodes via a facile hydrothermal method, in which the Cu/Ni-based nanotubes work as the “core” and porous  $\text{MnO}_2$  nanosheets serve as the “shell”. The unique core-shell nanostructure can benefit the improvements on the electrochemical properties of the electrode. Naturally, the core-shell nanostructure exhibits a high specific capacitance ( $374 \text{ F g}^{-1}$  at current density of  $0.25 \text{ A g}^{-1}$ ), good cycling stability (86.9% retention after 3000 cycles), and

\* Corresponding author at: College of Material Science and Engineering, Chongqing University, Chongqing 400044, PR China.

\*\* Corresponding author.

E-mail addresses: [xqqi@cqu.edu.cn](mailto:xqqi@cqu.edu.cn) (X.Q. Qi), [zhangyuxin@cqu.edu.cn](mailto:zhangyuxin@cqu.edu.cn) (Y.X. Zhang).

remarkable rate capability. It is believed that the nanocomposites would be a promising electrode material for energy storage devices.

## 2. Experimental

### 2.1. Materials synthesis

All the reagents in the experiments were of analytical purity and used without any further purification.

#### 2.1.1. Synthesis of Cu/Ni nanowires

In a typical synthesis [24], 15 ml NaOH (7 M) and 0.15 ml ethylenediamine (EDA) were mixed sufficiently in a reactor. Then, 0.26 ml  $\text{Ni}(\text{NO}_3)_2 \cdot 6\text{H}_2\text{O}$  (0.5 M) and 0.14 ml  $\text{Cu}(\text{NO}_3)_2 \cdot 6\text{H}_2\text{O}$  (0.5 M) were added and shaken until it turned blue, following by the sequential addition of 15 ml NaOH (7 M) and 0.15 ml hydrazine hydrate. Finally, the mixture was put into a Teflon-lined stainless steel autoclave maintained at 80 °C for 2 h. The precipitate was washed and dried at 60 °C in a vacuum for 12 h.

#### 2.1.2. Synthesis of Cu/Ni-based manganese dioxide

Briefly, Cu/Ni NWs (20 mg) were dissolved into 35 ml of 0.5 M  $\text{KMnO}_4$  solution to form homogeneous solution, and the mixture was transferred to a 50 ml Teflon-lined stainless steel autoclave which was sealed and maintained 140 °C for 24 h. In the end, the samples were washed several times and dried at 60 °C in a vacuum for 12 h.

### 2.2. Materials characterization

The compositions of the samples were characterized by powder X-ray diffraction (XRD, D/max 2500, Cu  $\text{K}\alpha$ ) and X-ray photoelectron spectroscope (XPS, Kratos XSAM800). The morphology and structure were observed by focused ion beam scanning electron microscopy (ZEISS AURIGA FIB/SEM) equipped with an energy dispersive X-ray spectrometer (EDS) and transmission electron microscopy (TEM, ZEISS LIBRA 200). The nitrogen adsorption-desorption isotherms were measured at 77 K by using micromeritics ASAP 2020 sorptometer.

### 2.3. Electrochemical measurements

All the electrochemical measurements were carried out in 1 M  $\text{Na}_2\text{SO}_4$  solution by using an electrochemical workstation (CHI 660E) in a three-electrode system. The saturated calomel (SCE) was

worked as the reference electrode and platinum plate was used as the counter electrode. A nickel foam ( $1 \times 1 \text{ cm}^2$ ) coated by the slurry was used as working electrode, which was composed of active materials, carbon black, and polyvinylidene fluoride (PVDF) with proportion of 7: 2: 1. The active materials were about 2.3 mg. The electrochemical impedance spectroscopy (EIS) was performed with a perturbation amplitude of 5 mV in the frequency between 100 kHz and 0.01 Hz. The specific capacitances are calculated according to the following equation [25]:

$$C_m = \frac{I\Delta t}{m\Delta V}$$

where  $I$  is the discharge current (A),  $\Delta t$  is the discharge time (s),  $m$  is the weight (g) of active materials, and  $\Delta V$  is the discharging potential window (V).

## 3. Results and Discussion

In order to confirm the composition and phase purity of the sample, XRD patterns of Cu/Ni-based manganese dioxide are shown in Fig. 1. It is clear that the diffraction peaks of Cu and Ni phases are in accord with the values in the standard card (Cu: JCPDS card no. 89-2838; Ni: JCPDS card no. 87-0712). [24] Meanwhile, the diffraction peaks of the CuO and NiO are well in line with the standard XRD patterns (CuO: JCPDS card no. 48-1548; NiO: JCPDS card no. 47-1049). The three strong diffraction peaks of the  $\text{MnO}_2$  at about 12.5°, 25.2° and 65.6° are indexed to (001), (002) and (020) planes of birnessite-type  $\text{MnO}_2$  (JCPDS card no. 80-1098) [21]. Obviously, no other diffraction peaks are detectable, indicating the high purity of the sample. Furthermore, the SEM image and corresponding EDS mapping of Cu/Ni-based manganese dioxide are shown in Fig. 2. As can be seen from the pictures, Cu, Ni, Mn and O elements are well distributed in the structure. Apparently, Cu and Ni elements are internally distributed, demonstrating the core-shell nanostructure. The strong C signal is observed because of the carbon-conducting tap for sample uploading. These results further confirm the composition of the sample.

To better understand the chemical composition and oxidation states, XPS spectra of the composite is presented in Fig. 3. The Mn 2p XPS spectrum displays two major peaks with a spin-energy separation of 11.8 eV (Fig. 3a) [21]. Fig. 3b shows XPS of Ni 2p core level at binding energy of 871.9 and 860.5 eV, confirming the oxide in the sample as NiO. The peak at 854.7 eV is connected with Ni. In the Cu 2p spectrum, two peaks at binding energy of 954.2 and 934.4 eV are corresponding to Cu 2p<sub>1/2</sub> and Cu 2p<sub>3/2</sub>. On the other

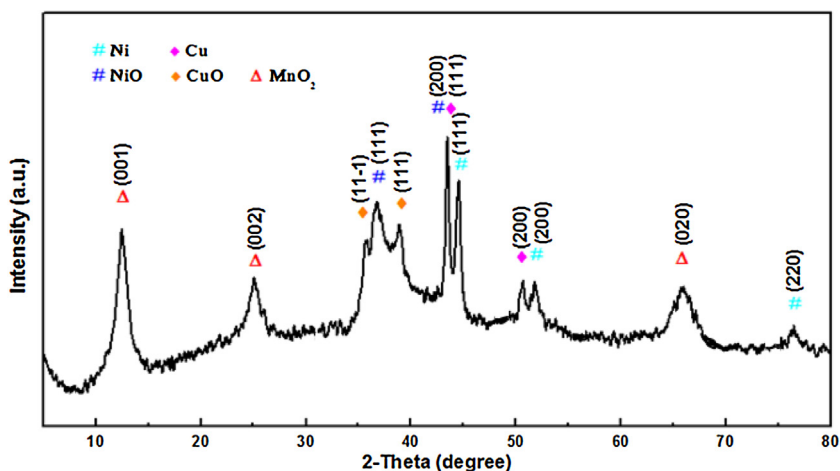


Fig. 1. XRD patterns of Cu/Ni-based manganese dioxide.

Download English Version:

<https://daneshyari.com/en/article/6606225>

Download Persian Version:

<https://daneshyari.com/article/6606225>

[Daneshyari.com](https://daneshyari.com)